LITHOS 526-527 (2026) 108443

Contents lists available at ScienceDirect

LITHOS

journal homepage: www.elsevier.com/locate/lithos

Not all that's high is sediment: Conflicting evidence for sediment assimilation in intrusive rocks of the Frontenac terrane, Grenville province

Gideon Asomani-Darko [a,*], Christopher J. Spencer [a], Nick M.W. Roberts [b], Evelyne Leduc [a], Emma Pluister [a]

[a] Department of Geological Sciences and Geological Engineering, Queen's University, Kingston, Ontario, Canada
[b] Geochronology and Tracers Facility, British Geological Survey, Nottingham, UK

ARTICLE INFO

Keywords:
Intrusive rocks
Assimilation
Altered Volcanic Rocks
High δ18O
Frontenac Terrane
Pelite

ABSTRACT

Crustal contamination during magma differentiation commonly involves the assimilation of pelitic sediments. Such assimilation typically increases peraluminosity and $\delta^{18}O$ of the resulting melt, leading to the widespread interpretation that high $\delta^{18}O$ signatures in igneous rocks reflect the assimilation of sediment. However, in the Frontenac terrane of the Grenville Province, metaluminous intrusive rocks display $\delta^{18}O$ values substantially higher than those of the mantle (~8–16.2‰), despite lacking peraluminous compositions, which complicates this interpretation. Contrary to previous proposals, we hypothesize that these high $\delta^{18}O$ values can be explained entirely through the incorporation of altered mafic igneous rocks rather than sedimentary materials, and this is supported by the lack of correlation between aluminosity and $\delta^{18}O$. In addition to the elevated $\delta^{18}O$ (~11.9 ± 2‰), we also report primary fluid inclusion isotopic signatures showing depleted $\delta^{13}C$ (−9.7 ± 4‰) and mantle-like $\delta^{2}H$ (−56.2 ± 10‰). These $\delta^{13}C$ and $\delta^{2}H$ isotopic characteristics are inconsistent with pelite assimilation but are compatible with the partial melting of altered mafic lithologies in the presence of carbon-depleted fluids, potentially sourced from serpentinized ultramafic rocks. This alternative explanation challenges the prevailing assumption that high $\delta^{18}O$ values in granitoids necessarily reflect sediment assimilation. Our results highlight the need to integrate elemental, isotopic, and geological evidence when interpreting magmatic contamination processes.

1. Introduction

The incorporation of supracrustal materials into magma can significantly alter its composition. However, identifying specific contaminants remains challenging due to the overlapping compositional signatures of geologic materials, thereby complicating efforts to understand granitoid petrogenesis. To address these complexities, various compositional proxies have been proposed, offering systematic frameworks to help identify the origin and evolution of granitoid magmas.

This study utilizes existing granitoid elemental and isotopic proxies (Chappell and White, 2001a; Taylor, 1978) to constrain the petrogenesis of the intrusive rocks in the Frontenac terrane. The Grenville Province of North America comprises reworked Archean to Proterozoic continental crust, along with new arc-related crust formed during the Mesoproterozoic, leading to the assembly of the supercontinent Rodinia (Dalziel et al., 2000; Easton, 1992; Rivers, 2008). The prolonged magmatism was marked by phases of arc accretion, syn to post-tectonic magmatism, and high-grade metamorphism (Carr et al., 2000; Easton, 1992).

The southwestern Grenville Province encompasses the Central Metasedimentary Belt (CMB), a ~ 28,500 km^2 region with diverse geology. This belt hosts numerous granitic plutons interspersed with metasedimentary units (Fig. 2). The Frontenac terrane of the (CMB) consists of Grenville supergroup metasedimentary and plutonic rocks that span ~1.19–1.08 Ga (Lumbers et al., 1990; Marcantonio et al., 1990; Peck et al., 2004). The dominant lithologies of the Frontenac terrane include magmatic rocks, viz., granite, syenite, quartz monzonite, syeno-diorite, granodiorite, and gabbro, along with marble and metapelite (Supplementary Fig. 1).

Oxygen isotopic studies of the granitoids in the CMB document elevated $\delta^{18}O$ values ranging from ~7.5‰ to ~14.5‰ (VSMOW) (Marcantonio et al., 1990; Peck et al., 2004; Shieh, 1985). Notably, the Frontenac terrane exhibits distinctly higher $\delta^{18}O$ signatures compared to the adjacent domains, as illustrated in Fig. 6A. Previous work has posited that the assimilation of basement gneisses, metapelite, and

* Corresponding author.
E-mail address: gideon.asomanidarko@queensu.ca (G. Asomani-Darko).

https://doi.org/10.1016/j.lithos.2026.108443
Received 9 October 2025; Received in revised form 1 February 2026; Accepted 1 February 2026
Available online 5 February 2026

marbles led to the high $\delta^{18}O$ signatures in the terrane (Marcantonio et al., 1990; Shieh, 1985). Importantly, the assimilation of metapelitic rocks would produce granitoids with higher peraluminousity. The intrusive rocks of the Frontenac terrane are, however, metaluminous rather than peraluminous. This discrepancy challenges existing models for granitoid petrogenesis, where high $\delta^{18}O$ signatures are attributed to the incorporation of metasedimentary rocks and raises critical questions about the factors controlling melt chemistry in this setting.

In this study, we integrate mineralogy, major element compositions, silicate oxygen isotopes, and both hydrogen and carbon isotopes of quartz-hosted fluid inclusions. We hypothesize that the composition of the Frontenac Terrane intrusive rocks can be best explained without any assimilation of metasedimentary rocks, but rather through the melting of altered oceanic crust and/or serpentinized ultramafic rocks during their formation. We further propose that the findings of this work serve as a caution against simplistic assumptions about magma-sediment interactions, commonly inferred from the $\delta^{18}O$ of detrital zircon.

2. Geological framework

The Grenville Province records multiple orogenic events (Shawinigan, Ottawan, and Rigolet orogenic phases) from ~1250 Ma to ~970 Ma, resulting in polymetamorphic amphibolite to granulite facies terranes that were intruded by compositionally diverse magmas (McLelland et al., 2010; Rivers, 2008; Rivers et al., 1989). The province represents tectonically stacked Mesoproterozoic thrust slices assembled during the Grenville orogeny. This orogeny is responsible for the deformation and metamorphism of the central metasedimentary belt (Davidson, 1984; McEachern and van Breemen, 1993; Rivers, 1997; Rivers et al., 1989). Before ~1180 Ma, the province experienced back-arc extension marked by elevated heat flow, crustal thinning, and calc-alkaline magmatism (Rivers, 1997). Magmatism during ~1180–1120 Ma led to the emplacement of the AMCG (anorthosite, mangerite, charnockite, granodiorite) suites, which include gabbroic to granitic plutons and widespread mafic dykes and sills (Augland et al., 2015; Rivers, 1997). The distribution of these rocks reflects ongoing mantle and crustal contributions to magmatism during this interval (Rivers, 1997).

2.1. Orogenic architecture of the southwestern Grenville province

The southwestern Grenville province is subdivided into two major tectonostratigraphic domains: the Central Metasedimentary Belt (CMB) and the Central Gneiss Belt (CGB) (Fig. 1B) (Carr et al., 2000). The CGB, dominated by Paleoproterozoic and Mesoproterozoic rocks, comprises distinct tectonic units separated by shear zones and faults, reflecting multiple episodes of continental collision, crustal thickening, and tectonic reworking during the Grenville orogeny. In contrast, the CMB includes the Composite Arc Belt and the Frontenac-Adirondack Belt and consists of a complex assemblage of volcanic and sedimentary rocks subdivided into several terranes and domains. These rocks have experienced metamorphism ranging from greenschist to granulite facies and have been intruded by various granitic to gabbroic plutons (Easton, 1992). The CGB and CMB are distinguished by differences in metamorphic grade, geochronology, and lithology. Geochronological data indicate that the CGB is significantly older (~1800–1400 Ma) compared to the CMB (~1300–1100 Ma) (Carr et al., 2000). Metamorphic grade generally increases from east to west across the province, with the CMB exhibiting lower-grade metamorphism.

2.1.1. The frontenac terrane

The Frontenac terrane, situated within the CMB, occupies a structurally complex position between the Adirondack Lowlands and the Maberly Shear Zone (Fig. 2). This terrane is characterized by a suite of syenite and monzonite plutonic rocks, emplaced between ~1.18 and 1.08 Ga (Lumbers et al., 1990;Marcantonio et al., 1990; Peck and Lin, 2025). These intrusions are hosted by granulite-facies metasedimentary rocks, including quartzofeldspathic and pelitic gneisses, marbles, and quartzite, with protolith ages ranging from ~1.19 to 1.16 Ga (Marcantonio et al., 1990; Peck and Lin, 2025). During the Shawinigan orogenic phase (~1180–1148 Ma), granitic magmas intruded the Proterozoic basement and earlier metasedimentary assemblages (Rivers, 2012). The Rideau-Canoe Lake fault separates the terrane into northern and southern domains (Fig. 2). According to Peck et al. (2004) the northern domain, hosts plutons comparable to the Kensington-Skootamatta suite (~1.09–1.08 Ga), whereas the southern domain includes older intrusions such as the Rockport Granite (~1.17 Ga) and granitoids of the Frontenac Terrane (~1.18–1.15 Ga). The study area spans both domains and includes a range of plutons, including the

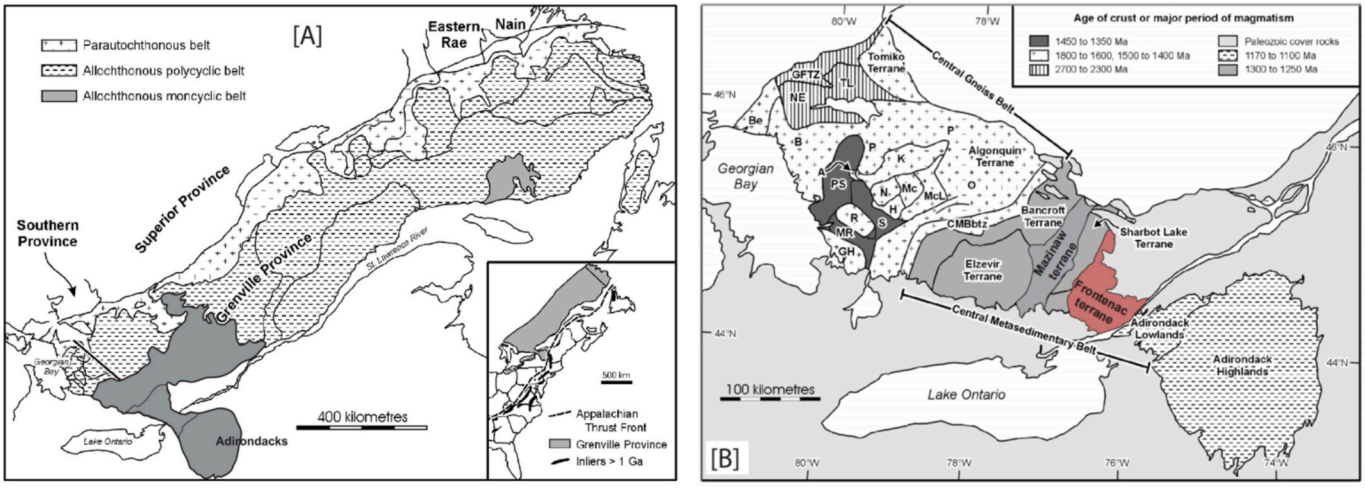

Fig. 1. Geology of the Grenville province. [B] Subdivisions of the Southwestern Grenville province showing the study area in red. Figures used after (Carr et al., 2000). Abbreviations: A, Ahmic domain; B, Britt domain; BD, Belmont domain; Be, Beverstone domain (part of Killarney magmatic belt); BT, Bancroft domain; CMBbtz, Central Metasedimentary Belt boundary thrust zone; G, Grimsthorpe domain; GFTZ, Grenville Front tectonic zone; GH, Go Home domain; H, Huntsville domain; HC, Harvey Cardiff Arch; K, Kiosk domain; Mc, McCraney domain; McL, McLintock domain; MR, Moon River domain; MT, Mazinaw terrane; N, Novar domain; NE, Nepewassi domain; O, Opeongo domain; P, Powassan domain; PS, Parry Sound domain; R, Rosseau domain; S, Seguin domain; SD, Shawanaga domain; SL, Sharbot Lake domain; TL, Tilden Lake domain. (For interpretation of the references to colour in this figure legend, the reader is referred to the web version of this article.)

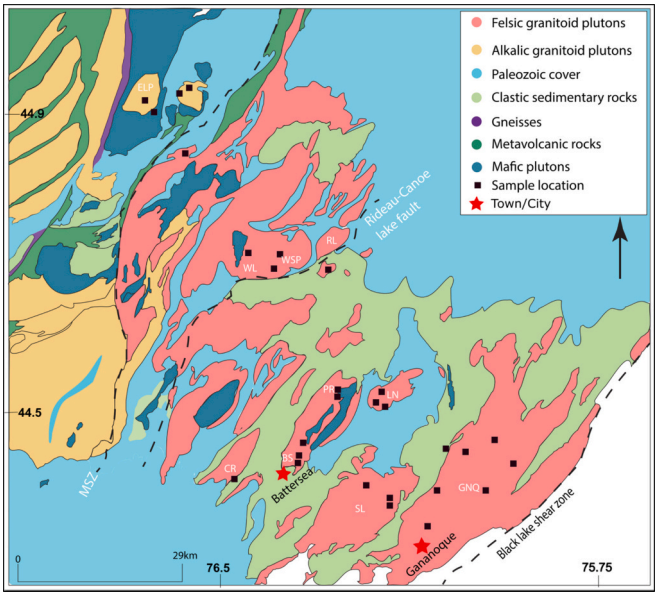

Fig. 2. Geological map of the Frontenac terrane showing the major plutons from which samples were collected. Abbreviations: WL. Wolfe Lake, WSP. Westport, R.L. Rideau Lake, PR. Perth Road, LN. Lyndhurst, CR. Crow Lake, BS. Battersea, SL. South Lake, GNQ. Gananoque.

northern plutons: the Elphin, Westport, Wolfe-Lake, and Rideau Lake, and the southern region plutons, including the Crow Lake, Perth Road Syenite, Lyndhurst, Battersea, South Lake, and Gananoque plutons. These intrusions comprise a diverse lithological assemblage, including syenite, monzonite, quartz monzonite, tonalite, granite, and granodiorite. The plutons are structurally concordant with older gabbroic bodies but exhibit localized evidence of metasomatic alteration. This spatial and structural relationship suggests a post-emplacement interaction between the intrusive magmas and the mafic crust, likely influencing the mineralogical and textural variation. The gabbros are typically massive, fine- to medium-grained, and equigranular, composed primarily of plagioclase feldspar and pyroxene, with minimal quartz.

Syenite and syeno-monzonite plutons are volumetrically dominant and are mineralogically defined by 30–60% orthoclase, 15–30% pyroxene and other mafic minerals, and variable quartz (typically <5% to 15%). Pegmatitic syenites with potassium feldspar and pyroxene crystals exceeding 4 cm are locally observed. Tonalites are coarse-grained, light grey to white, primarily composed of plagioclase and quartz with ~10–20% mafic minerals. Though generally lacking penetrative deformation, syenite bodies locally intrude the gabbros as dykes or irregular plutons, commonly with sharp intrusive contacts. The presence of pyroxene xenocrysts in some syenites suggests magma interaction with gabbroic host rocks, and migmatitic textures in certain zones imply partial melting (Supplementary Fig. 2). Together, these intrusive relationships, xenocrystic textures, and metasomatic features support a multiphase magmatic history in which syenitic melts exploited and interacted with pre-existing mafic crust.

3. Methods

3.1. Major element composition

Reagent-grade nitric and hydrochloric acids (VWR chemicals) were pre-purified in-house using a sub-boiling Savillex DST-1000 distillation system. For sample digestion, 4.5 mL concentrated HNO_3, 1.5 mL concentrated HCl and 2 mL ultrapure 50% HF (VWR chemicals) were added to 100 mg of sample weighed into Teflon microwave digestion vessels. The samples were then digested in an Anton Parr Multiwave 5000 microwave reaction system using a 20SVT50 rotor, where temperatures were increased to 220 °C, and the sample vessels were allowed to react for 20 min. The digested samples were transferred into clean Savillex containers and evaporated overnight on a hotplate at 85 °C in a Class 100 clean laboratory. An addition of 2 mL of cleaned 1.28% boric acid and ~ 500 μL of concentrated HCl was made to the drying samples, which were then left to react for several hours, capped on an 85 °C hot plate to remove any fluorides produced during digestion. Samples were fully dried down overnight and diluted in 2% HNO_3. Samples were sonicated to ensure all material was dissolved and filtered to 0.45 μm for analysis. The diluted samples were analyzed using a Thermo Scientific iCAP PRO Series inductively coupled plasma-optical emission spectrometer (ICP-OES) coupled with a 4DX Elemental Scientific prepFAST M5 autosampler for sample introduction and dilution. BHVO-1 and GSP-1 were used as reference materials. Sample introduction and operating conditions are displayed in *Supplementary Table 3*.

3.2. Silicate oxygen isotopes ($\delta^{18}O$)

Selected quartz grains and whole rock samples (Frontenac terrane intrusive rocks) were pulverized, and 5–6 mg of the resultant powder was used for the analyses. Samples were loaded in the silicate extraction line. Oxygen from the silicate minerals is extracted using the BrF_5 method and converted to CO_2 through interaction with red-hot graphite (Clayton and Mayeda, 1963). Isotopic analysis of CO_2 gas was conducted via dual inlet on a ThermoFisher Scientific Delta^{Plus}XP Isotope-Ratio Mass Spectrometer (IRMS). $\delta^{18}O$ is reported relative to Vienna Standard Mean Ocean Water (VSMOW), in permil units (‰). Analytical uncertainty is 0.4‰. The silicate reference sample NBS28 and Anglo Basalt were routinely included in the analytical procedure.

3.3. Carbon ($\delta^{13}C$) and hydrogen ($\delta^{2}H$) isotopes of quartz-hosted fluid inclusions

Quartz separates containing fluid inclusions were analyzed for $\delta^{13}C$. Individual quartz crystals from each sample were grain-picked, and ~ 40 mg were weighed into tin capsules and loaded into a zero-blank autosampler on a Costech ECS 4010 Elemental Analyzer (EA) coupled to a ThermoFisher Scientific Delta^{Plus}XP Continuous-Flow Isotope Ratio Mass Spectrometer (CF-IRMS) via a Conflo III at the Queen's Facility for Isotope Research (QFIR), Kingston, Ontario, Canada. The samples were combusted at 1050 °C, and the resulting gas mixture was reduced at 650 °C before undergoing separation in a chromatography oven at 80 °C. The $\delta^{13}C$ values of the generated CO_2 are reported using the delta (δ) notation in permil (‰) and calibrated against VPDB and VSMOW, respectively, with precisions of 0.2‰. The isotopic reference material used for these analyses was NBS21 graphite, and a sulfanilamide compositional standard was also measured to quantify the C concentration in the samples.

For the hydrogen isotopes, 40 mg of selected quartz separates containing fluid inclusions were weighed into silver capsules and heated at 100 °C for 1 h to remove adsorbed moisture. Degassed samples were loaded into the zero-blank autosampler of a ThermoFisher Scientific TC/EA High Temperature Conversion Elemental Analyzer coupled to a ThermoFisher Scientific MAT 253 Stable Isotope Ratio Mass Spectrometer via a Conflo IV. Samples were pyrolyzed at 1450 °C, decomposing individual grains and releasing hydrogen-bearing fluids as H_2 gas. $\delta^{2}H$ values are reported using delta (δ) notation in permil (‰), relative to Vienna Standard Mean Ocean Water (VSMOW), with a precision of 3‰. Certified reference materials USGS 57 and USGS 58 were used to ensure the quality of the analyses.

4. Results

Major oxides show that the samples have compositions of monzonite, quartz-monzonite, granite, granodiorite, syenite, quartz syenite and with just a few being tonalite (Debon and Fort, 1983) (*Supplementary*

Table 2). Based on A/CNK ratios, most samples are peralkaline to metaluminous, and two samples are weakly peraluminous (Fig. 3A). The A/B diagram (Fig. 3D) confirms the petrographic observations as it shows clinopyroxene and amphibole as the dominant mafic minerals.

K_2O contents vary between 1 and 8 wt%, peaking in samples with 70–80 wt%SiO_2. Most of the samples plot within and above the high-K calc-alkaline series of granitoids (Fig. 3B). The intrusive rocks exhibit bimodal mafic element (Mg + Fe + Ti) compositions and are categorized into high and low-mafic groups, though their Mg/(Fe + Mg) ratios remain relatively uniform (Fig. 3C). Notably, the majority of the analyzed samples cluster within the low-mafic compositional group.

Isotopic data from representative plutons in the Frontenac terrane are presented in Table 1. Quartz $\delta^{18}O$ values range from 8.0‰ to 16.2‰ (average: 12.0‰), while whole-rock values span from 6.9‰ to 14.1‰ (average: 11.0‰). The $\delta^{18}O$ values obtained from whole-rock and quartz samples were compared against compiled zircon $\delta^{18}O$ data from the Adirondacks (4.31–9.91‰; average: 8.7‰). All datasets consistently yield $\delta^{18}O$ values significantly higher than typical mantle-derived crustal signatures (6.0–7.5‰) (Fig. 5).

While whole-rock and quartz compositions are often susceptible to secondary hydrothermal alteration, zircon is notably resistant to isotopic exchange after crystallization. The fact that the zircon data reflect the enriched signatures found in both the whole-rock and quartz datasets suggests that the high $\delta^{18}O$ values represent a primary feature of the source rock rather than post-magmatic processes. Also, the possibility of significant oxygen exchange through wall-rock alteration was previously evaluated by Shieh (1985). The findings indicated that such interactions were insignificant in this region, further supporting the conclusion that these elevated isotopic signatures are inherent to the lithological suite.

A spatial trend is evident (Marcantonio et al., 1990; Shieh, 1985), with $\delta^{18}O$ values decreasing northward toward the Maberly Shear Zone (MSZ), marking the northern boundary of the Frontenac terrane. $\delta^{2}H$ values range from −80.0‰ to −42‰ (VSMOW) and $\delta^{13}C$ values span

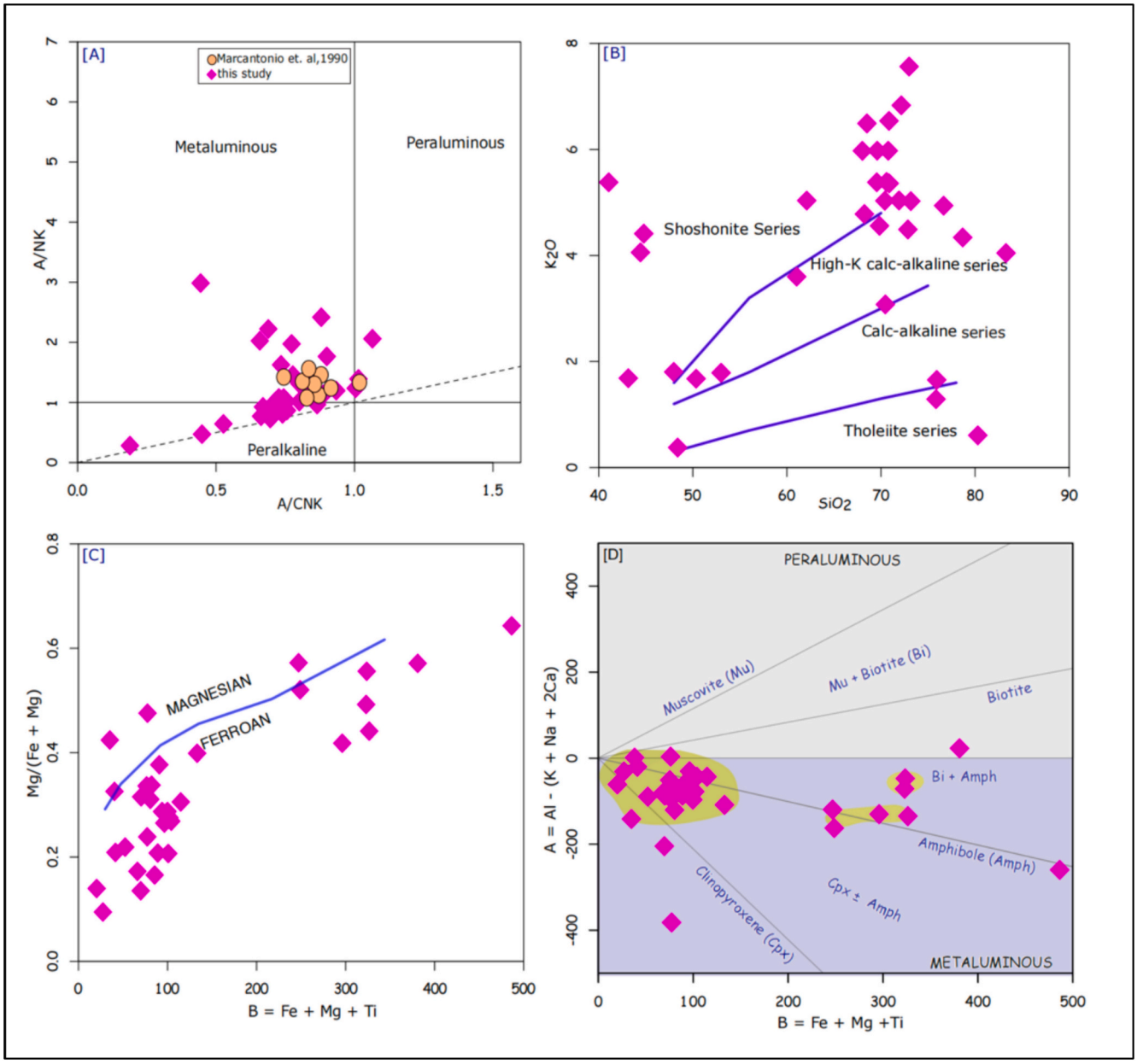

Fig. 3. Geochemistry of the Frontenac terrane granitoids. [A] A/NK vs. A/CNK plot after (Shand, 1927), [B] K_2O vs. SiO_2 discriminant diagram (Peccerillo and Taylor, 1976), [C] Ferroan plot (Debon and Fort, 1983) and [D] A vs. B diagram after (Debon and Fort, 1983).

Table 1
Sample location and stable isotopic data for intrusive rocks of the Frontenac terrane, Ontario, Canada.

Sample ID	Pluton/Domain	$\delta^{18}O$ ‰ vs VSMOW	$\delta^{2}H$ ‰ vs VSMOW	$\delta^{13}C$ ‰ vs VPDB	C wt%	Lat.	Long.
GAD31A	Battersea	13.3	−80	−15.4	0.03	44.45244	−76.35821
GAD32	Battersea	11.9	−41.5	−16.6	0.01	44.44261	−76.36156
GAD30	Crow lake	13.4	−51.3	−12.6	0.03	44.42563	−76.48239
EBL13B	Elphin	11.9	−56.2	−9.7		44.89723	76.60725
GAD01	Elphin	14.1	–	–	–	44.91498	−76.62739
GAD02	Elphin	8.3	−68.6	−6.8		44.89946	−76.61021
GAD03	Elphin	10.9	−46.8	−13.2		44.92937	−76.54187
GAD04	Elphin	12	−59.3	−7.5		44.92270	−76.56087
EBL02	Gananoque	10.5	–	–	–	44.43803	−75.94318
EBL07	Gananoque	11.3	–	–	–	44.44706	−76.24791
GAD19A	Gananoque	14.7	−60.6	−14.2	0.02	44.35394	−76.12030
GAD19C	Gananoque	14.2	−66.3	−6.9	0.03	44.35394	−76.12030
GAD22	Gananoque	9	−63	−15.4	0.02	44.44834	−76.04399
GAD23	Gananoque	12	−54.5	−5.4	0.05	44.44834	−76.04399
EBL06	Lyndhurst	14.4	–	–	–	44.53294	−76.25363
GAD26	Lyndhurst	10.5	−49.4	−14	0.02	44.51643	−76.20938
GAD27	Lyndhurst	9.9	−46.3	−5.1	0.05	44.52931	−76.19804
GAD28A	Lyndhurst	16.2	−51.2	−2.9	0.09	44.53304	−76.27984
GAD32B	Perth road	–	−60	−14.6	0.02	44.42563	−76.48239
GAD33	Perth road	–	−65.3	−10.7	0.02	44.42598	−76.48790
GAD34A	Perth road	12.4	−43	−13.6	0.02	44.42612	−76.48796
GAD13	Rideau lake	11.6	–	–	–	44.68858	−76.29007
GAD14	Rideau lake	9.7	–	–	–	44.68858	−76.29007
EBL11	Sharbot lake	6.9		−12.8	0.03	44.81391	−76.52351
EBL14A	Sharbot lake	8.2	–	−10.2	0.01	44.67043	−76.67471
EBL14B	Sharbot lake	8.2	–	−7	0.05	44.67043	−76.67471
GAD9A	Sharbot lake	9.5	−53.7	−5.7		44.80802	−76.51615
GAD9B	Sharbot lake	9.5	−49.6	−7.1		44.80802	−76.51615
GAD9C	Sharbot lake	9.5	−52.7	−7.5		44.80802	−76.51615
EBL05	South lake	11.1	–	–	–	44.52228	−76.17069
EBL4A	South lake	14.1	–	−21.8	0.01	44.54143	−76.13728
GAD15	South lake	13.2	−63.3	−10.6	0.02	44.41021	−76.23424
GAD17	South lake	13.9	−46.4	−6.8	0.03	44.39282	−76.19040
GAD11	Wolfe lake	10.5	–	−25.5		44.69254	−76.39294

−25.5‰ to −2.9‰ (VPDB).

SiO_2 content across the CMB ranges from 40 to 78 wt% (Fig. 6A). The sample distribution shows a distinct correlation between $\delta^{18}O$ and SiO_2 in the CMB. Formation of granitoids through normal fractional crystallization of mantle-sourced magma yields $\delta^{18}O$ of ~7.5‰ with a SiO_2/$\delta^{18}O$ slope of 0.06 (Fig. 6B).

As illustrated in Fig. 6C, ASI shows a systematic decrease with progressive magmatic fractionation, consistent with the depletion of aluminum relative to silica during crystallization. In contrast, Fig. 6D reveals no correlation between ASI and $\delta^{18}O$ values within the Frontenac terrane. This decoupled behaviour implies that aluminosity and oxygen isotope signatures are governed by distinct magmatic processes or source reservoirs.

5. Discussion

Geochemical proxies (e.g., major element compositions, oxygen isotopes ($\delta^{18}O$)) are commonly used alongside mineralogical data to establish the petrogenesis of intrusive rocks. The formation of such rocks involves complex processes, including sediment contamination and magma mixing during their magmatic evolution. Intrusive felsic rocks that have differentiated (through partial melting and/or fractional crystallization) from mantle-derived magmas are commonly classified as I-types. These granitoids typically exhibit a low alumina saturation index (ASI < 1.0, based on molar A/CNK values) (Chappell and White, 2001a, 2001b), hence the term, metaluminous (Shand, 1927). They are also characterized by orthopyroxene, hornblende, epidote, and calcium/potassium-rich plagioclase feldspar mineral assemblages (Kemp and Hawkesworth, 2003; Shand, 1927) with $\delta^{18}O$ values typically less than 7.8‰ (Taylor, 1968).

In contrast, intrusive felsic rocks formed through the melting and assimilation of supracrustal rocks, particularly sediments, are classified as S-types (ASI > 1) and are typically peraluminous (Chappell and White, 2001a, 2001b; Shand, 1927). They are also characterized by minerals such as garnet, muscovite, and cordierite, and exhibit $\delta^{18}O$ values typically >8.4‰ (Bucholz and Spencer, 2019; Kemp and Hawkesworth, 2003; Taylor, 1968). Problematic to the I- vs. S-type classification is that it has variable use among different authors; it can be based on mineralogy, geochemistry, inferred magmatic source, or a combination of these.

Although 1) the original S-type classification inferred a source incorporating sedimentary material (Chappell and White, 2001a, 2001b), and 2) elevated $\delta^{18}O$ signatures ($\delta^{18}O$ > 8.4‰) common to S-type granitoids can be explained by sediment incorporation, these signatures are not solely attributable to this mechanism. Along with sediment assimilation, the incorporation of altered volcanic rocks can also contribute to this isotopic enrichment (Taylor, 1978). We argue that researchers commonly overlook the contribution of altered volcanic rocks, thereby oversimplifying the origin of high $\delta^{18}O$ signatures by attributing them exclusively to the incorporation of sediments.

In the Frontenac terrane, the intrusive rocks are predominantly metaluminous in composition and are consistent with the definition of I-type granitoids (Fig. 3A) as stated by (Shand (1927); Chappell and White (2001a, 2001b); Kemp and Hawkesworth (2003)). To characterize these rocks and understand their petrogenesis, their major elemental composition was examined (*Supplementary Table 2)*. Examining these compositions allows us to move beyond their broad classification (I-type) and purposefully discuss these rocks based on their chemical signatures, peculiar to their evolution in the Frontenac terrane. Upon analysis, these samples exhibit anomalously high K_2O concentrations (Fig. 3B), which may be attributed to two primary mechanisms, viz., derivation from a potassium-rich source rock and post-magmatic alteration.

We suggest that partial melting or assimilation of potassium-rich

mafic to intermediate protoliths, such as basaltic andesites or andesites, could account for the elevated K_2O concentrations observed in these samples. Potential sources of high-K volcanic rocks are present in the nearby Mazinaw-Elzevir terrane, viz., the Tudor Formation (1.29 Ga) and the overlying Kashwakamak Formation (Harnois and Moore, 1991). These subalkaline basalts and andesites are depleted in Nb and Ti with enrichment in Sr, Rb, Ba and K. These characteristics are most consistent with arc-derived volcanic rocks (Harnois and Moore, 1991). Our hypothesis of the assimilation of K-rich mafic rocks (Tudor and Kashwakamak formations) is supported because both formations predate the evolution of Frontenac intrusive rocks.

Dry partial melting of lower crustal rocks (Tudor and Kashwakamak formations), combined with fractionation of clinopyroxene, amphibole, and other ferromagnesian minerals, may have driven potassium and sodium enrichment in the residual melts. This process would draw Ca, Mg, and Fe into crystallizing phases, leaving the melt enriched in alkalis (Fig. 4) (Roberts and Clemens, 1993). This model aligns with the observed minor occurrences of peralkaline signatures, which are typically associated with shallow crustal fractionation under anhydrous conditions (Bailey, 1974). A dry melting environment in the lower crust would suppress the stability of hydrous minerals, promoting alkali retention and enrichment in the melt (Bailey, 1974).

The character of the metavolcanic rocks described above provides a potential solution to the elevated $\delta^{18}O$ that we find in the intrusive rocks of the Frontenac terrane. The Frontenac terrane is distinguished by much higher $\delta^{18}O$ values, averaging 12‰ vs. VSMOW and exhibits contrasting magmatic sources. High-silica magmas with low $\delta^{18}O$ signatures coexist with intermediate-silica magmas characterized by elevated $\delta^{18}O$ signatures (Fig. 6A). This implies a contribution from diverse crustal and mantle sources. All plutons in the FT display $\delta^{18}O$ values above the typical mantle-derived magmatic trend (Fig. 6B), thereby classifying the entire terrane as a high-$\delta^{18}O$ domain (Taylor, 1968). The observed variability in both SiO_2 and $\delta^{18}O$ within the terrane underscores complex magmatic processes, likely involving assimilation, fractional crystallization and potential mixing of isotopically distinct sources. εNd values presented by (Marcantonio et al., 1990) on the Frontenac terrane intrusive rocks range from −6 to +3.1. These values reflect both crustal and mantle influence in the formation of the rocks, hence supporting our claim of complex magmatic processes. A mantle source containing 40 wt% silica and a $\delta^{18}O$ value of 5.5‰ can generate felsic magma through fractional crystallization, during which $\delta^{18}O$ progressively increases to ~7.5‰ (Fig. 6B) (Bindeman et al., 2004; Bucholz et al., 2017). However, the slope of fractionation of the lowest-$\delta^{18}O$ intrusive rocks in the terrane is twice the normal mantle-derived

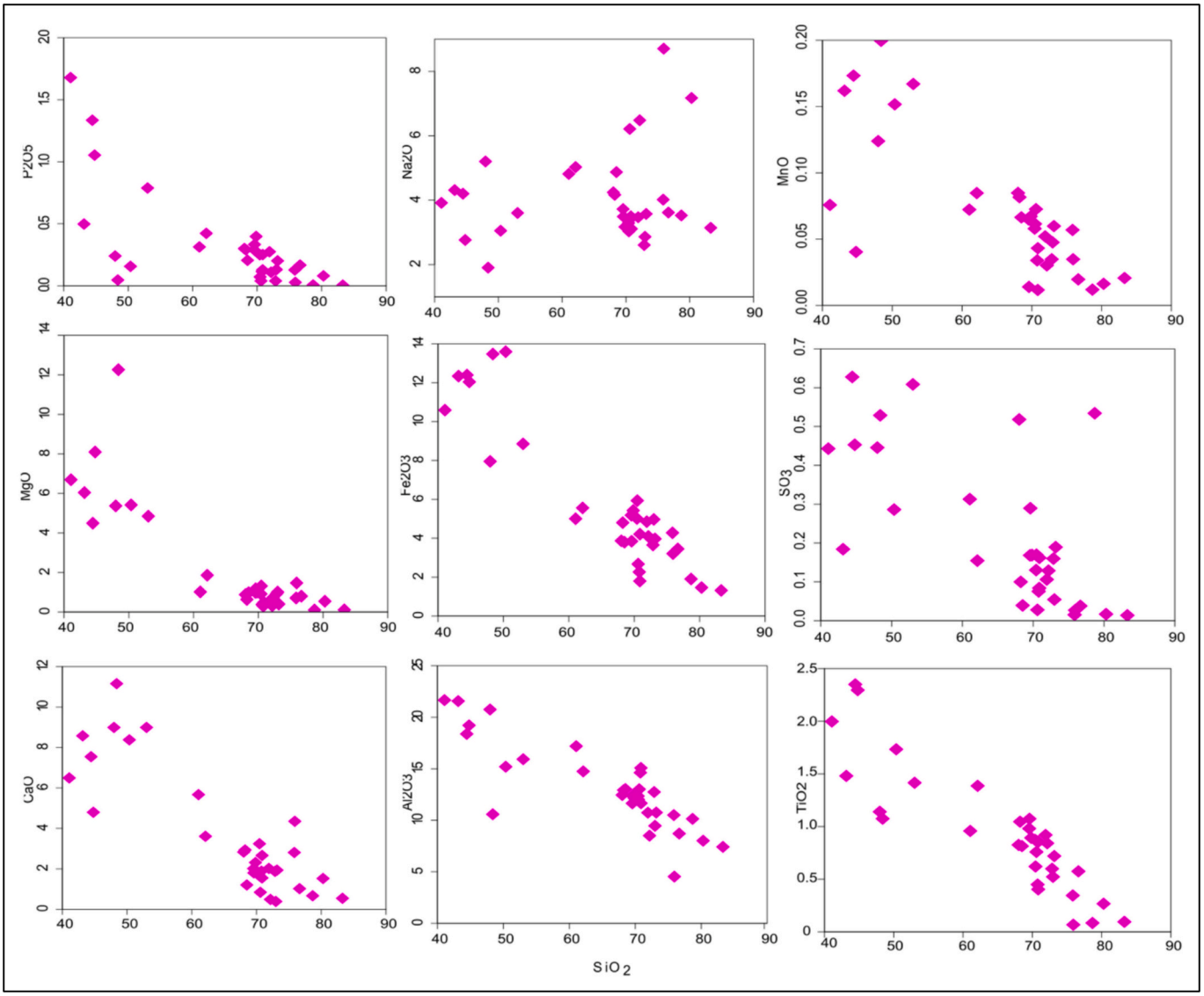

Fig. 4. [a]-[i] variation diagram of major elements against SiO_2 for Frontenac terrane intrusive rocks.

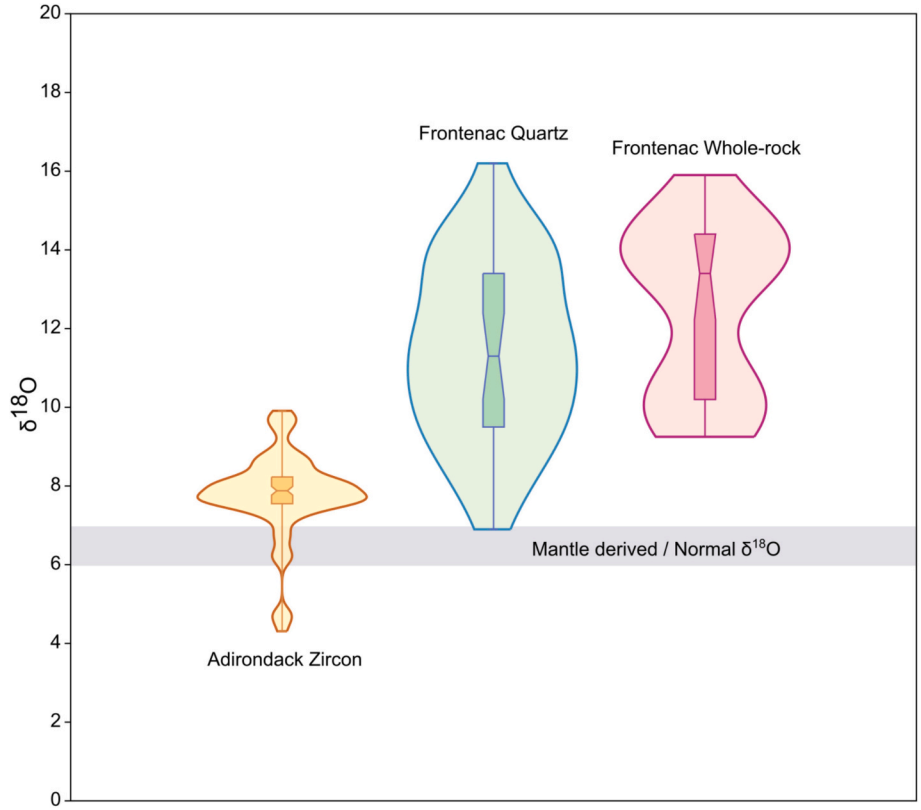

Fig. 5. Comparison of zircon $\delta^{18}O$ values from the Adirondacks (Valley et al., 1994) with quartz (this study) and whole-rock (Peck et al., 2004) $\delta^{18}O$ data. All samples exhibit values significantly higher than those of mantle-derived $\delta^{18}O$.

fractionation trend, indicating that the generation of the higher-$\delta^{18}O$ intrusive rocks is not possible through simple fractional crystallization of a mantle source alone. Therefore, we must examine the possibility of mixing between two magma sources and of assimilation. The mixing lines presented in Fig. 7 demonstrate that primary metaluminous composition is preserved when ~30% pelite is assimilated, resulting in a $\delta^{18}O$ of ~8.7‰. At ~35% assimilation, strongly peraluminous melts are produced with $\delta^{18}O$ values of ~9.4‰. Greywackes follow a similar trend, with 30% assimilation producing intrusive rocks with $\delta^{18}O$ values of ~9‰. In contrast, partial melting of AVR does not increase the aluminosity beyond metaluminous compositions yet yields $\delta^{18}O$ values exceeding 9‰. These findings support our hypothesis that the intrusive rocks in the Frontenac terrane were formed via the assimilation of altered volcanic rock rather than metasedimentary materials.

Although our bulk-mixture modelling treats ASI as reflecting the relative proportions of source materials, we note that subsequent fractional crystallization and mineral assemblage evolution can modify ASI away from the initial source-mix value, potentially enhancing peraluminosity. These findings nevertheless support our hypothesis that the intrusive rocks in the Frontenac terrane were formed via the assimilation of altered volcanic rock rather than metasedimentary materials.

A recent study focused on understanding deep carbon recycling, Li et al. (2019) provided a significant piece of evidence as part of their findings. The study revealed extensive isotopic heterogeneity where the range of isotopic signatures of AVR spans ~8 to ~35‰ ($\delta^{18}O$) and − 25 to +5‰ ($\delta^{13}C$). With AOC being the primary reservoir, which is subducted into the mantle (Keller et al., 2024), it shows that assimilating AOC/AVR can introduce the necessary isotopically heavy oxygen (^{18}O) and light carbon (^{12}C) into a magmatic source. The assimilation of a magmatic source containing recycled high $\delta^{18}O$ and depleted $\delta^{13}C$ AVR/AOC into an evolving magma can directly affect the signatures of the resultant granitoid.

We posit that the melting and assimilation of high-$\delta^{18}O$ supracrustal materials such as AVR accounts for the elevated oxygen isotope signatures observed in the Frontenac terrane without significantly increasing the peraluminosity of the intrusive rocks. Modern AVR is commonly enriched in ^{18}O due to low-temperature interaction with seawater yet remains consistent with major-element compositions with mantle-derived magmas. Hence, the assimilation of AVR will impart elevated $\delta^{18}O$ signatures to the evolving melt while preserving its metaluminosity, which is consistent with the signatures of the Frontenac terrane intrusive rocks.

The depleted $\delta^{13}C$ and mantle-like $\delta^{2}H$ signatures in the Frontenac terrane intrusive rocks (Fig. 8 A) are likely not attributable to a single source, as no clear correlation exists between the isotopic signatures of the mantle and altered oceanic crust end members. The lack of a clear trend between the mantle and AOC may imply a heterogeneous magma source. We infer that isotopic fractionation occurred during serpentinization of existing mafic rocks (e.g., gabbro) and the subsequent release of fluids.

Evidence for the serpentinization of mafic rocks (e.g., metagabbro) near Perth, situated in the Frontenac terrane, has been detailed by Freeman (1954). During serpentinization, methane (CH_4) and molecular hydrogen (H_2), which result in more negative $\delta^{13}C$ and $\delta^{2}H$, are generated (de Obeso et al., 2022), and interaction of these fluids with the evolving magma may have shifted the isotopic signatures away from mantle values. This process, coupled with assimilation of AOC, provides a plausible mechanism for the observed $\delta^{13}C$, $\delta^{2}H$, and carbon content variations in the intrusive rocks. The $\delta^{13}C$ values of the Frontenac intrusive rocks range from −2.5‰ to −27‰ (VPDB), decreasing systematically with carbon content (Fig. 8B). The relationship between organic and total carbon concentrations suggests negligible input of inorganic carbon in the samples. Similar $\delta^{13}C$ trends documented in the Oman listvenites (products of ultramafic rock alteration) (de Obeso et al., 2022) support the hypothesis that similar serpentinization-driven processes influenced the Frontenac terrane intrusive rocks. Importantly,

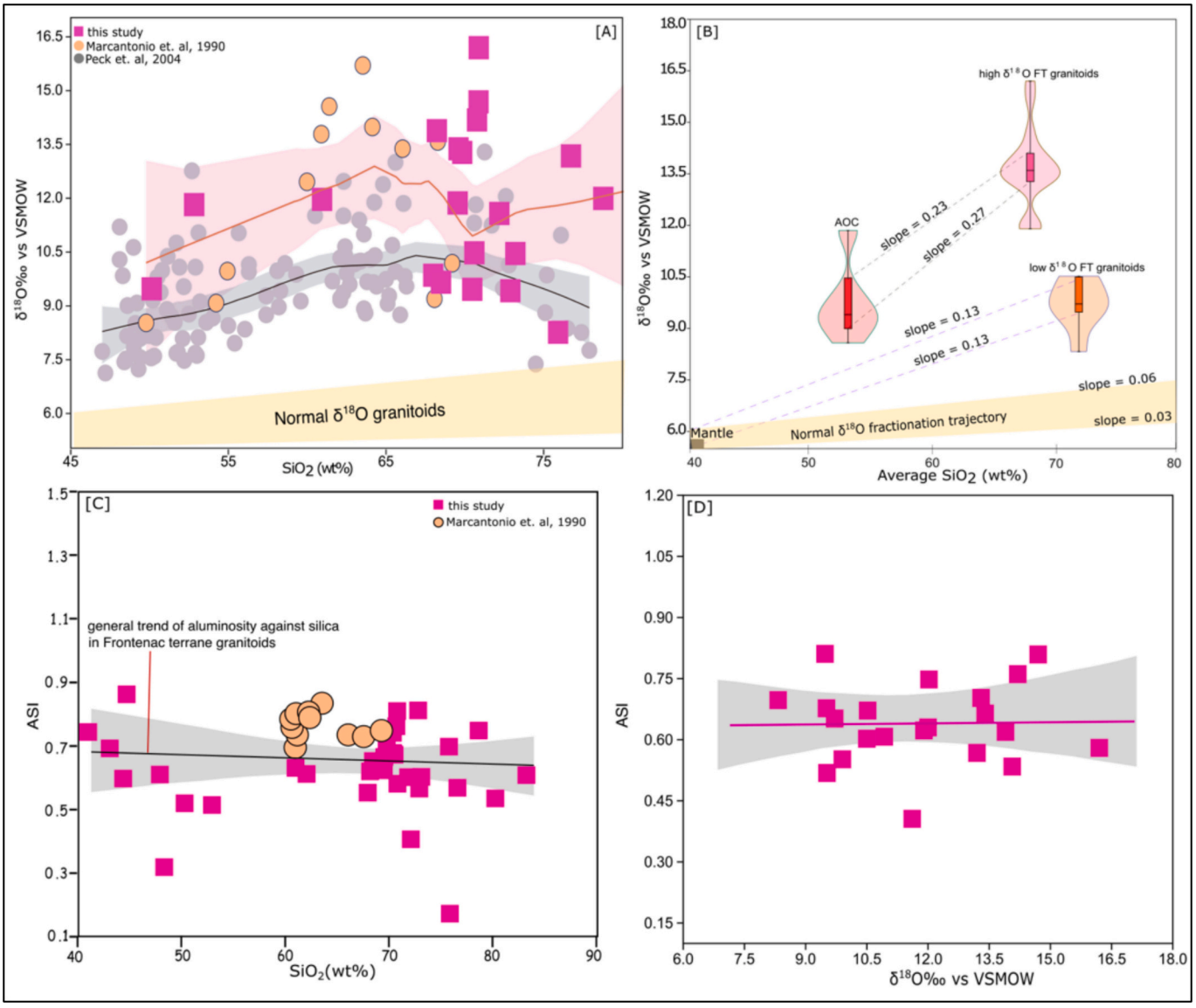

Fig. 6. [A] $\delta^{18}O$ vs. SiO_2 plot of the CMB. [B] $\delta^{18}O$ vs. SiO_2 plot illustrating oxygen isotope variability within the Frontenac terrane. The *yellow* and grey circles represent data from (Marcantonio et al., 1990; Peck et al., 2004), respectively. *The shaded areas correspond to a LOESS bootstrap with a 0.3 smoothing factor.* Normal $\delta^{18}O$ fields (Bindeman et al., 2004; Bucholz et al., 2017). [C] Relationship between aluminosity and silica as magma fractionates. [D] Aluminosity against $\delta^{18}O$ shows no systematic correlation between the entities. *The grey shaded areas represent 95% bootstrap.* (For interpretation of the references to colour in this figure legend, the reader is referred to the web version of this article.)

these interpretations involve not only bulk assimilation of AOC but also the incorporation of isotopically distinctive fluids released during serpentinization, both of which can leave distinct signatures in isotopes and whole-rock geochemistry.

6. Implications

The assumption that sediments are the only source of high $\delta^{18}O$ in intrusive rocks has fostered the axiom: elevated $\delta^{18}O$ must result from sediment melting (Gao et al., 2022; Guo et al., 2012; Hopkinson et al., 2017; Kemp et al., 2007; Lackey et al., 2006; Spencer et al., 2017; Wang et al., 2020). This assumption underpins many models of granitoid petrogenesis and influences how detrital zircon $\delta^{18}O$ is interpreted.

Detrital zircon offers the most comprehensive long-term magmatic record of Earth's evolution due to its exceptional ability to preserve isotopic signatures over geological timescales (Gehrels, 2014). Their unique physical and chemical durability enables zircon to endure repeated tectonothermal events, thereby recording magmatic events from the Hadean to the present (Andersen et al., 2016; Fedo et al., 2003; Finch and Hanchar, 2003; Gehrels, 2014). This robustness renders detrital zircon records an invaluable asset when evaluating crustal evolution (Barham et al., 2022; Cawood et al., 2012).

Using $\delta^{18}O$ in detrital zircon records serves as an important tool in discriminating igneous protoliths and magma sources (Spencer et al., 2022). Any significant shift from the pristine mantle ($5.3 \pm 0.6‰$; Valley et al., 1998, 2005) is generally interpreted due to the influence of sedimentary materials, given the large difference in $\delta^{18}O$ between sediments and the mantle (Kemp et al., 2006; Liebmann et al., 2021; Spencer et al., 2022). High $\delta^{18}O$ magmas are generally thought to be restricted to the upper crust and are predominantly produced by the assimilation of metasedimentary rocks and are therefore more likely to be included in the sedimentary record (Spencer et al., 2022).

An interpretive bias toward assuming sedimentary assimilation is evident in a systematic review of zircon $\delta^{18}O$ literature from the Puetz et al. (2024) database, which shows that of 377 studies, nearly half (185) report zircon $\delta^{18}O$ values exceeding 7.5‰, a threshold unlikely to result

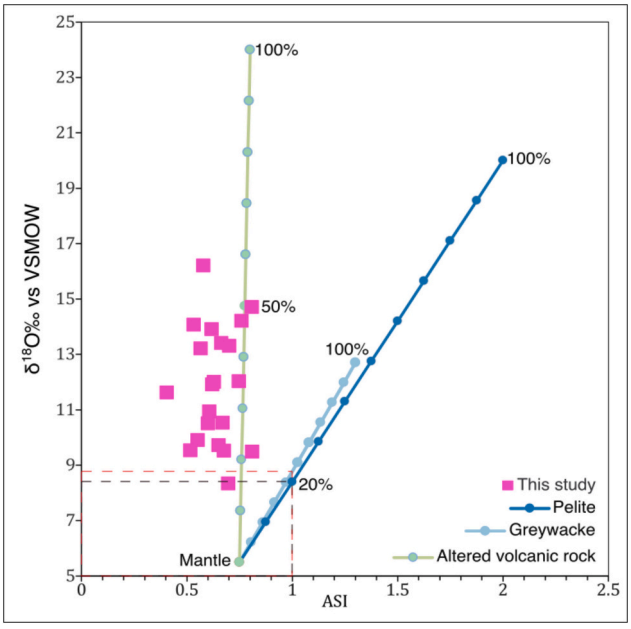

Fig. 7. ASI vs $\delta^{18}O$ (‰ vs VSMOW) mixing curve for basaltic to rhyolitic magmas. Lines denote theoretical mixing between mantle and crustal end members. Average greywacke, pelite and AVR end members are from (Bindeman et al., 2016; Hill et al., 1981 & Li et al., 2019), respectively. Dashed lines show 30% mixing of Pelite and Greywacke and their corresponding $\delta^{18}O$ yield.

from normal magmatic fractionation alone (Bindeman et al., 2004; Bucholz et al., 2017). Of these, 128 are studies reporting igneous zircon, and 57 relate to detrital zircon. Authors predominantly attribute high $\delta^{18}O$ to sediment assimilation: 56% of igneous studies and 54% of detrital studies cited sediments as the source, compared to just 17% and 9%, respectively, that considered altered volcanic rocks (Fig. 9A & B). The remainder invoked a non-specific "supracrustal" source. Critically, among the detrital zircon studies that attributed high $\delta^{18}O$ to sediment assimilation, only 42% reported inherited cores that would substantiate sediment incorporation; the remaining 58% did not (Fig. 9C). This raises concern that sediment assimilation is being over-assumed in cases where altered mafic sources, capable of generating similar $\delta^{18}O$ values, may be equally or more plausible but remain underappreciated. These findings urge caution in assigning $\delta^{18}O$ signatures to specific crustal reservoirs without supporting textural or isotopic evidence, especially in detrital zircon studies where contextual constraints are inherently limited.

Granitoids formed in sediment-rich convergent plate margins (like the Himalayan orogeny) typically show elevated $\delta^{18}O$ signatures (>8‰) due to assimilation of high $\delta^{18}O$ sedimentary materials (Gao et al., 2022; Hopkinson et al., 2017). This association has shaped prevailing interpretations of ancient zircon $\delta^{18}O$ records, reinforcing a default link between high $\delta^{18}O$ and sediment involvement. For example, the rise in zircon $\delta^{18}O$ during the early Proterozoic has been widely interpreted as a signal of enhanced sediment subduction and melting during early global plate tectonics (Bahlburg et al., 2025; Bindeman et al., 2022; Spencer et al., 2022; Valley et al., 2005). However, this framework commonly assumes a singular petrogenetic process, despite increasing evidence that other lithologies can impart similar isotopic signals.

Recent work by Lu et al. (2024) on the petrogenesis of high $\delta^{18}O$ A_2-type granitoids hypothesized that this shift can be linked to diverse high $\delta^{18}O$ source components, such as the partial melting of altered oceanic crust in a retreating back-arc setting, and not solely subducted sediments. Vaguely applying the principle of uniformitarianism risks oversimplifying Precambrian tectonics, neglecting non-subduction mechanisms such as squishy-lid geodynamic processes, plume-related magmatic underplating, and whole-rock and isotopic geochemistry (Sm—Nd, Lu—Hf) (Liu et al., 2024; Lu et al., 2024).

7. Conclusions

Whole-rock major element geochemistry confirms the metaluminous nature of the Frontenac terrane intrusive rocks, which display elevated $\delta^{18}O$ values ranging from ~8 to 16.2‰, with an average of 12‰. The accompanying biogenic $\delta^{13}C$ and depleted $\delta^{2}H$ signatures are consistent with assimilation of AOC in the presence of a $\delta^{13}C$-depleted fluid, potentially derived from serpentinized ultramafic rocks. Together, these data suggest that the observed isotopic signatures can be generated without invoking sedimentary assimilation, challenging prevailing models that link elevated $\delta^{18}O$ values directly to pelitic input. We

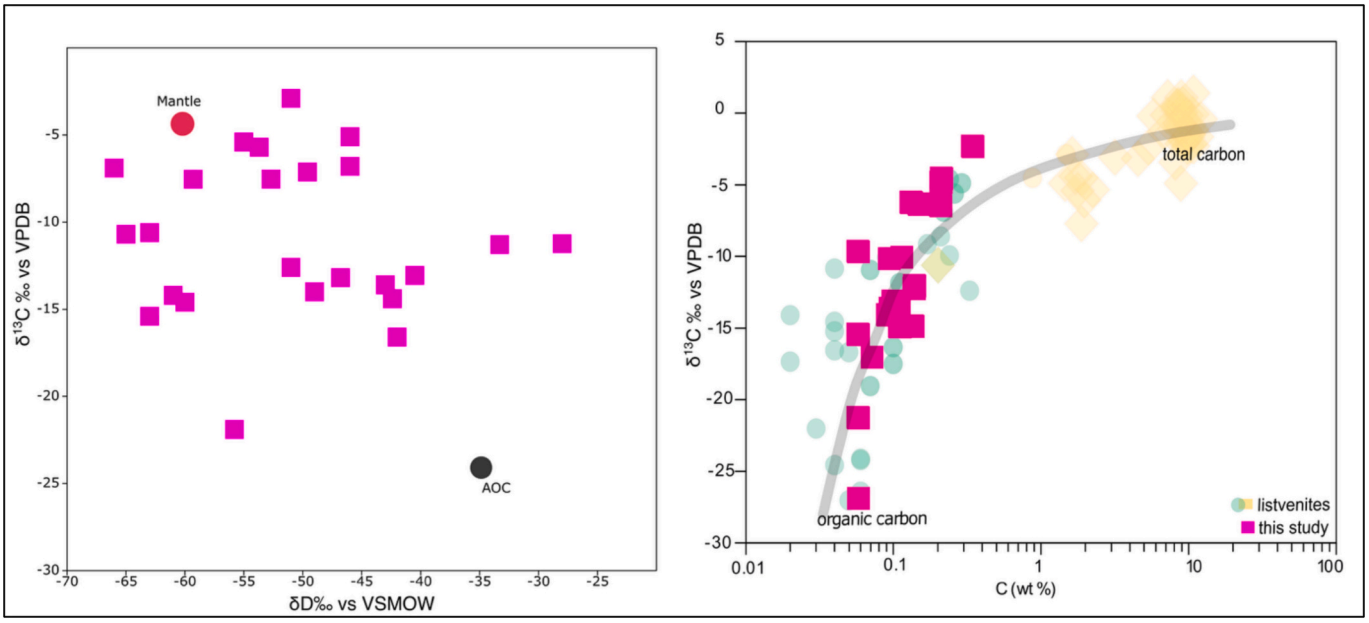

Fig. 8. [A] Plot of $\delta^{13}C$ (‰ vs VPDB) against $\delta^{2}H$ (‰ vs VSMOW) in Frontenac granitoids. [B] $\delta^{13}C$ against total and organic carbon for Frontenac granitoids and Oman Listvenites. Listvenite's data from (de Obeso et al., 2022).

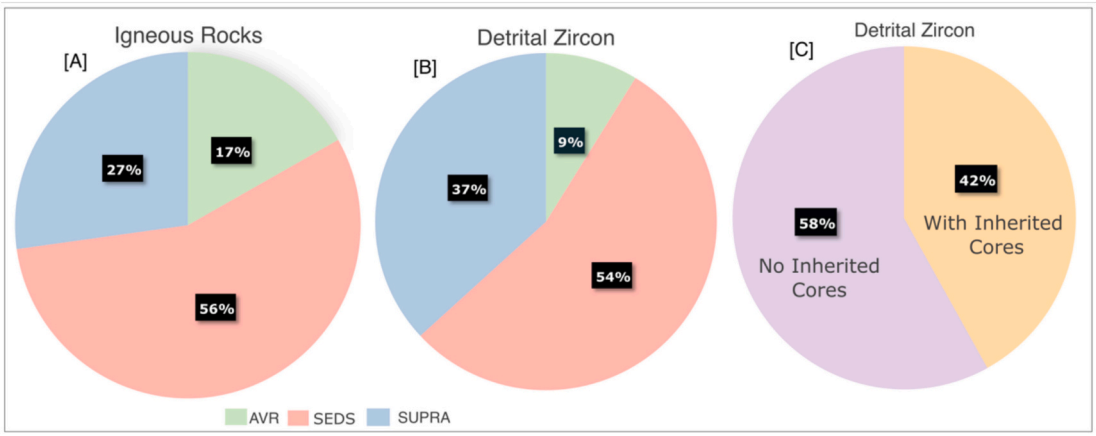

Fig. 9. Summary of published studies invoking contaminants to explain high $\delta^{18}O$ signatures. [A–B] Sediments are cited as the sole contaminant in 56% of igneous petrogenesis studies and 54% of detrital zircon investigations. [C] Inherited cores, indicative of sediment recycling, are discussed in 42% of detrital zircon studies. Data from Puetz et al. (2024).

therefore propose a critical re-evaluation of the widespread assumption that high $\delta^{18}O$ values in granitoids, and particularly in detrital zircon, necessarily reflect sedimentary protoliths. Instead, our findings suggest that high $\delta^{18}O$ signatures may also arise from magmatic systems that interact with altered mafic lithologies and associated fluids. Recognizing this alternative model to explain elevated $\delta^{18}O$ magmas has significant implications for interpreting crustal evolution, as it broadens the range of tectonic settings and processes capable of producing high-$\delta^{18}O$ magmas and complicates the direct attribution of such signatures to supracrustal recycling.

CRediT authorship contribution statement

Gideon Asomani-Darko: Writing – review & editing, Writing – original draft, Visualization, Validation, Project administration, Methodology, Investigation, Formal analysis, Data curation, Conceptualization. **Christopher J. Spence:** Writing – review & editing, Validation, Supervision, Project administration, Methodology, Funding acquisition, Conceptualization. **Nick M.W. Roberts:** Writing – review & editing, Validation. **Evelyne Leduc:** Writing – review & editing, Methodology. **Emma Pluister:** Methodology.

Declaration of competing interest

The authors declare the following financial interests/personal relationships which may be considered as potential competing interests.

Gideon Asomani-Darko reports financial support was provided by Natural Sciences and Engineering Research Council of Canada. If there are other authors, they declare that they have no known competing financial interests or personal relationships that could have appeared to influence the work reported in this paper.

Appendix A. Supplementary data

Supplementary data to this article can be found online at https://doi.org/10.1016/j.lithos.2026.108443.

References

Andersen, T., Kristoffersen, M., Elburg, M.A., 2016. How far can we trust provenance and crustal evolution information from detrital zircons? A South African case study: Gondwana Research 34, 129–148. https://doi.org/10.1016/j.gr.2016.03.003.

Augland, L.E., Moukhsil, A., Solgadi, F., Indares, A., 2015. Pinwarian to Grenvillian magmatic evolution in the Central Grenville Province: new constraints from ID–TIMS U–Pb ages and coupled Lu–Hf S–MC–ICP–MS data. In: McFarlane, C. (Ed.), Canadian Journal of Earth Sciences, v. 52, pp. 701–721. https://doi.org/10.1139/cjes-2014-0232.

Bahlburg, H., Kemp, A.I.S., Fanning, C.M., Martin, L., 2025. The Hf and O isotope record of long-lasting accretionary orogens: the example of the Proterozoic and Paleozoic-Triassic Central South America. Earth-Sci. Rev. 262, 105068. https://doi.org/10.1016/j.earscirev.2025.105068.

Bailey, D.K., 1974. Experimental petrology relating to oversaturated peralkaline volcanics: a review. Bull. Volcanol. 38, 637–652. https://doi.org/10.1007/BF02596901.

Barham, M., Kirkland, C.L., Handoko, A.D., 2022. Understanding ancient tectonic settings through detrital zircon analysis. Earth Planet. Sci. Lett. 583, 117425. https://doi.org/10.1016/j.epsl.2022.117425.

Bindeman, I.N., Ponomareva, V.V., Bailey, J.C., Valley, J.W., 2004. Volcanic arc of Kamchatka: a province with high-δ18O magma sources and large-scale 18O/16O depletion of the upper crust1. Geochim. Cosmochim. Acta 68, 841–865. https://doi.org/10.1016/j.gca.2003.07.009.

Bindeman, I.N., Bekker, A., Zakharov, D.O., 2016. Oxygen isotope perspective on crustal evolution on early Earth: a record of Precambrian shales with emphasis on Paleoproterozoic glaciations and Great Oxygenation Event. Earth Planet. Sci. Lett. 437, 101–113. https://doi.org/10.1016/j.epsl.2015.12.029.

Bindeman, I.N., Ionov, D.A., Tollan, P.M.E., Golovin, A.V., 2022. Oxygen isotope (δ18O, Δ′17O) insights into continental mantle evolution since the Archean: Nature. Communications 13, 3779. https://doi.org/10.1038/s41467-022-31586-9.

Bucholz, C.E., Spencer, C.J., 2019. Strongly Peraluminous Granites across the Archean–Proterozoic transition. J. Petrol. 60, 1299–1348. https://doi.org/10.1093/petrology/egz033.

Bucholz, C.E., Jagoutz, O., VanTongeren, J.A., Setera, J., Wang, Z., 2017. Oxygen isotope trajectories of crystallizing melts: Insights from modeling and the plutonic record. Geochim. Cosmochim. Acta 207, 154–184. https://doi.org/10.1016/j.gca.2017.03.027.

Carr, S.D., Easton, R.M., Jamieson, R.A., Culshaw, N.G., 2000. Geologic transect across the Grenville orogen of Ontario and New York1. Can. J. Earth Sci. 37, 193–216. https://doi.org/10.1139/e99-074.

Cawood, P.A., Hawkesworth, C.J., Dhuime, B., 2012. Detrital zircon record and tectonic setting. Geology 40, 875–878. https://doi.org/10.1130/G32945.1.

Chappell, B.W., White, A.J.R., 2001a. Two contrasting granite types: 25 years later. Aust. J. Earth Sci. 48, 489–500. https://doi.org/10.1046/j.1440-0952.2001.00882.x.

Chappell, B.W., White, A.J.R., 2001b. Two contrasting granite types: 25 years later. Aust. J. Earth Sci. 48, 489–499. https://doi.org/10.1046/j.1440-0952.2001.00882.x.

Clayton, R.N., Mayeda, T.K., 1963. The use of bromine pentafluoride in the extraction of oxygen from oxides and silicates for isotopic analysis. Geochim. Cosmochim. Acta 27, 43–52. https://doi.org/10.1016/0016-7037(63)90071-1.

Dalziel, I.W.D., Mosher, S., Gahagan, L.M., 2000. Laurentia-Kalahari Collision and the Assembly of Rodinia. J. Geol. 108, 499–513. https://doi.org/10.1086/314418.

Davidson, A., 1984. Tectonic boundaries within the Grenville province of the Canadian shield. J. Geodyn. 1, 433–444. https://doi.org/10.1016/0264-3707(84)90018-8.

de Obeso, J.C., Kelemen, P.B., Leong, J.M., Menzel, M.D., Manning, C.E., Godard, M., Cai, Y., Bolge, L., Party, O.D.P.P. 1 S, 2022. Deep sourced fluids for peridotite carbonation in the shallow mantle wedge of a fossil subduction zone: Sr and C isotope profiles of OmanDP Hole BT1B. J. Geophys. Res. Solid Earth 127, e2021JB022704. https://doi.org/10.1029/2021JB022704.

Debon, F., Fort, P.L., 1983. A chemical–mineralogical classification of common plutonic rocks and associations. Earth Environ. Sci. Trans. R. Soc. Edinb. 73, 135–149. https://doi.org/10.1017/S0263593300010117.

Easton, R.M., 1992. The Grenville Province and the Proterozoic History of Central and Southern Ontario. Geology of Ontario, Ontario Geological Survey, Special.

Fedo, C.M., Sircombe, K.N., Rainbird, R.H., 2003. Detrital Zircon Analysis of the Sedimentary Record. Rev. Mineral. Geochem. 53, 277–303. https://doi.org/10.2113/0530277.

Finch, R.J., Hanchar, J.M., 2003. Structure and Chemistry of Zircon and Zircon-Group Minerals. Rev. Mineral. Geochem. 53, 1–25. https://doi.org/10.2113/0530001.

Freeman, P.V., 1954. A Petrological Study of the Munro Asbestos 'A' Orebody, Matheson, Ontario [M.Sc]. McGill University (Canada), p. 106. https://www.proquest.com/docview/2650266590/abstract/81C56A798CB247FCPQ/1 (accessed December 2025).

Gao, M.-H., Liu, P.-P., Chung, S.-L., Li, Q.-L., Wang, B., Tian, W., Li, X.-H., Lee, H.-Y., 2022. Himalayan zircons resurface in Sumatran arc volcanoes through sediment recycling. Commun. Earth Environ. 3, 283. https://doi.org/10.1038/s43247-022-00611-6.

Gehrels, G., 2014. Detrital Zircon U-Pb Geochronology Applied to Tectonics. Annu. Rev. Earth Planet. Sci. 42, 127–149. https://doi.org/10.1146/annurev-earth-050212-124012.

Guo, C., Chen, Y., Zeng, Z., Lou, F., 2012. Petrogenesis of the Xihuashan granites in southeastern China: Constraints from geochemistry and in-situ analyses of zircon UPbHfO isotopes. Lithos 148, 209–227. https://doi.org/10.1016/j.lithos.2012.06.014.

Harnois, L., Moore, J.M., 1991. Geochemistry of two metavolcanic arc suites from the Central Metasedimentary Belt of the Grenville Province, southeastern Ontario, Canada. Can. J. Earth Sci. 28, 1429–1443. https://doi.org/10.1139/e91-126.

Hill, M., Morris, J., Whelan, J., 1981. Hybrid granodiorites intruding the accretionary prism, Kodiak, Shumagin, and Sanak Islands, Southwest Alaska. J. Geophys. Res. Solid Earth 86, 10569–10590. https://doi.org/10.1029/JB086iB11p10569.

Hopkinson, T.N., Harris, N.B.W., Warren, C.J., Spencer, C.J., Roberts, N.M.W., Horstwood, M.S.A., Parrish, R.R., Eimf, 2017. The identification and significance of pure sediment-derived granites. Earth Planet. Sci. Lett. 467, 57–63. https://doi.org/10.1016/j.epsl.2017.03.018.

Keller, D.S., Lee, C.-T.A., Peck, W.H., Monteleone, B.D., Martin, C., Vervoort, J.D., Bolge, L., 2024. Mafic slab melt contributions to Proterozoic massif-type anorthosites: Science. Advances 10. https://doi.org/10.1126/sciadv.adn3976 p. eadn3976.

Kemp, A.I.S., Hawkesworth, C.J., 2003. 3.11 - Granitic Perspectives on the Generation and Secular Evolution of the Continental Crust. In: Holland, H.D., Turekian, K.K. (Eds.), Treatise on Geochemistry. Pergamon, Oxford, pp. 349–410. https://doi.org/10.1016/B0-08-043751-6/03027-9.

Kemp, A.I.S., Hawkesworth, C.J., Paterson, B.A., Kinny, P.D., 2006. Episodic growth of the Gondwana supercontinent from hafnium and oxygen isotopes in zircon. Nature 439, 580–583. https://doi.org/10.1038/nature04505.

Kemp, A.I.S., Hawkesworth, C.J., Foster, G.L., Paterson, B.A., Woodhead, J.D., Hergt, J. M., Gray, C.M., Whitehouse, M.J., 2007. Magmatic and Crustal Differentiation history of Granitic Rocks from Hf-O Isotopes in Zircon. Science 315, 980–983. https://doi.org/10.1126/science.1136154.

Lackey, J.S., Valley, J.W., Hinke, H.J., 2006. Deciphering the source and contamination history of peraluminous magmas using δ18O of accessory minerals: examples from garnet-bearing plutons of the Sierra Nevada batholith. Contrib. Mineral. Petrol. 151, 20–44. https://doi.org/10.1007/s00410-005-0043-6.

Li, K., Li, L., Pearson, D.G., Stachel, T., 2019. Diamond isotope compositions indicate altered igneous oceanic crust dominates deep carbon recycling. Earth Planet. Sci. Lett. 516, 190–201. https://doi.org/10.1016/j.epsl.2019.03.041.

Liebmann, J., Spencer, C.J., Kirkland, C.L., Xia, X.-P., Bourdet, J., 2021. Effect of water on δ18O in zircon. Chem. Geol. 574, 120243. https://doi.org/10.1016/j.chemgeo.2021.120243.

Liu, J., Palin, R.M., Mitchell, R.N., Liu, Z., Zhang, J., Li, Z., Cheng, C., Zhang, H., 2024. Archaean multi-stage magmatic underplating drove formation of continental nuclei in the North China Craton. Nat. Commun. 15, 6231. https://doi.org/10.1038/s41467-024-50435-5.

Lu, G.-M., Xu, Y.-G., Wang, W., Spencer, C.J., Roberts, N.M.W., Condie, K.C., 2024. Diverse source materials contributed to a secular increase in δ18O for the Paleo-Mesoproterozoic A2-type granites. Earth Planet. Sci. Lett. 642, 118885. https://doi.org/10.1016/j.epsl.2024.118885.

Lumbers, S.B., Heaman, L.M., Vertolli, V.M., Wu, T.W., Gower, C.F., Rivers, T., Ryan, A. B., 1990. Nature and timing of Middle Proterozoic magmatism in the Central Metasedimentary Belt, Grenville Province, Ontario: Mid-Proterozoic Laurentia–Baltica. In: Gower, C.F., Rivers, T., Ryan, A.B. (Eds.), Geol. Assoc. Can. Spec. Pap, 38, pp. 243–276.

Marcantonio, F., McNutt, R.H., Dickin, A.P., Heaman, L.M., 1990. Isotopic evidence for the crustal evolution of the Frontenac Arch in the Grenville Province of Ontario, Canada. Chem. Geol. 83, 297–314. https://doi.org/10.1016/0009-2541(90)90286-G.

McEachern, S.J., van Breemen, O., 1993. Age of deformation within the Central Metasedimentary Belt boundary thrust zone, Southwest Grenville Orogen: constraints on the collision of the Mid-Proterozoic Elzevir terrane. Can. J. Earth Sci. 30, 1155–1165. https://doi.org/10.1139/e93-098.

McLelland, J.M., Selleck, B.W., Bickford, M.E., 2010. Review of the Proterozoic evolution of the Grenville Province, its Adirondack outlier, and the Mesoproterozoic inliers of the Appalachians. In: from Rodinia to Pangea: the Lithotectonic Record of the Appalachian Region. Geological Society of America. https://doi.org/10.1130/2010.1206(02).

Peccerillo, A., Taylor, S.R., 1976. Geochemistry of eocene calc-alkaline volcanic rocks from the Kastamonu area, Northern Turkey. Contrib. Mineral. Petrol. 58, 63–81. https://doi.org/10.1007/BF00384745.

Peck, W.H., Lin, H.Y., 2025. Provenance and depositional age of metasedimentary rocks in the Frontenac terrane (Grenville Province, Ontario). Can. J. Earth Sci., cjes-2024-0029 https://doi.org/10.1139/cjes-2024-0029.

Peck, W., Valley, J., Corriveau, L., Davidson, A., Mclelland, J., Farber, D., 2004. Oxygen-isotope constraints on terrane boundaries and origin of 1.18–1.13 Ga granitoids in the southern Grenville Province. Mem. Geol. Soc. America v. 197. https://doi.org/10.1130/0-8137-1197-5.163.

Puetz, S.J., Spencer, C.J., Condie, K.C., Roberts, N.M.W., 2024. Enhanced U-Pb detrital zircon, Lu-Hf zircon, δ18O zircon, and Sm-Nd whole rock global databases. Sci. Data 11, 56. https://doi.org/10.1038/s41597-023-02902-9.

Rivers, T., 1997. Lithotectonic elements of the Grenville Province: Review and tectonic implications. Precambrian Res. 86, 117–154. https://doi.org/10.1016/S0301-9268(97)00038-7.

Rivers, T., 2008. Assembly and preservation of lower, mid, and upper orogenic crust in the Grenville Province—Implications for the evolution of large hot long-duration orogens. Precambrian Res. 167, 237–259. https://doi.org/10.1016/j.precamres.2008.08.005.

Rivers, T., 2012. Upper-crustal orogenic lid and mid-crustal core complexes: signature of a collapsed orogenic plateau in the hinterland of the Grenville Province 1This article is one of a series of papers published in CJES Special Issue: in honour of Ward Neale on the theme of Appalachian and Grenvillian geology. Can. J. Earth Sci. 49, 1–42. https://doi.org/10.1139/e11-014.

Rivers, T., Martignole, J., Gower, C.F., Davidson, A., 1989. New tectonic divisions of the Grenville Province, Southeast Canadian Shield. Tectonics 8, 63–84. https://doi.org/10.1029/TC008i001p00063.

Roberts, M.P., Clemens, J.D., 1993. Origin of high-potassium, calc-alkaline, I-type granitoids. Geology 21, 825–828. https://doi.org/10.1130/0091-7613(1993)021%3C0825:OOHPTA%3E2.3.CO;2.

Shand, S.J., 1927. Eruptive Rocks: Their Genesis, Composition, Classification, and their Relation to Ore-Deposits, with a Chapter on Meteorites. T. Murby & Company.

Shieh, Y.-N., 1985. High-18O granitic plutons from the Frontenac Axis, Grenville province of Ontario, Canada. Geochim. Cosmochim. Acta 49, 117–123. https://doi.org/10.1016/0016-7037(85)90195-4.

Spencer, C.J., Cavosie, A.J., Raub, T.D., Rollinson, H., Jeon, H., Searle, M.P., Miller, J.A., McDonald, B.J., Evans, N.J., the Edinburgh Ion Microprobe Facility (EIMF), 2017. Evidence for melting mud in Earth's mantle from extreme oxygen isotope signatures in zircon. Geology 45, 975–978. https://doi.org/10.1130/G39402.1.

Spencer, C.J., Cavosie, A.J., Morrell, T.R., Lu, G.M., Liebmann, J., Roberts, N.M.W., 2022. Disparities in oxygen isotopes of detrital and igneous zircon identify erosional bias in crustal rock record. Earth Planet. Sci. Lett. 577, 117248. https://doi.org/10.1016/j.epsl.2021.117248.

Taylor, H.P., 1968. The oxygen isotope geochemistry of igneous rocks. Contrib. Mineral. Petrol. 19, 1–71. https://doi.org/10.1007/BF00371729.

Taylor, H.P., 1978. Oxygen and hydrogen isotope studies of plutonic granitic rocks. Earth Planet. Sci. Lett. 38, 177–210. https://doi.org/10.1016/0012-821X(78)90131-0.

Valley, J.W., Chiarenzelli, J.R., McLelland, J.M., 1994. Oxygen isotope geochemistry of zircon. Earth Planet. Sci. Lett. 126, 187–206. https://doi.org/10.1016/0012-821X(94)90106-6.

Valley, J.W., Kinny, P.D., Schulze, D.J., Spicuzza, M.J., 1998. Zircon megacrysts from kimberlite: oxygen isotope variability among mantle melts. Contrib. Mineral. Petrol. 133, 1–11. https://doi.org/10.1007/s004100050432.

Valley, J.W., et al., 2005. 4.4 billion years of crustal maturation: oxygen isotope ratios of magmatic zircon. Contrib. Mineral. Petrol. 150, 561–580. https://doi.org/10.1007/s00410-005-0025-8.

Wang, C.-C., Jacobs, J., Elburg, M.A., Läufer, A., Elvevold, S., 2020. Late Neoproterozoic–Cambrian magmatism in Dronning Maud Land (East Antarctica): U–Pb zircon geochronology, isotope geochemistry and implications for Gondwana assembly. Precambrian Res. 350, 105880. https://doi.org/10.1016/j.precamres.2020.105880.